A Direct Measurement of the W Boson Width in $p\bar{p}$ Collisions at $\sqrt{s} = 1.96$ TeV

T. Aaltonen,[23] J. Adelman,[13] T. Akimoto,[54] M.G. Albrow,[17] B. Álvarez González,[11] S. Amerio,[42] D. Amidei,[34] A. Anastassov,[51] A. Annovi,[19] J. Antos,[14] M. Aoki,[24] G. Apollinari,[17] A. Apresyan,[47] T. Arisawa,[56] A. Artikov,[15] W. Ashmanskas,[17] A. Attal,[3] A. Aurisano,[52] F. Azfar,[41] P. Azzi-Bacchetta,[42] P. Azzurri,[45] N. Bacchetta,[42] W. Badgett,[17] A. Barbaro-Galtieri,[28] V.E. Barnes,[47] B.A. Barnett,[25] S. Baroiant,[7] V. Bartsch,[30] G. Bauer,[32] P.-H. Beauchemin,[33] F. Bedeschi,[45] P. Bednar,[14] D. Beecher,[30] S. Behari,[25] G. Bellettini,[45] J. Bellinger,[58] A. Belloni,[22] D. Benjamin,[16] A. Beretvas,[17] J. Beringer,[28] T. Berry,[29] A. Bhatti,[49] M. Binkley,[17] D. Bisello,[42] I. Bizjak,[30] R.E. Blair,[2] C. Blocker,[6] B. Blumenfeld,[25] A. Bocci,[16] A. Bodek,[48] V. Boisvert,[48] G. Bolla,[47] A. Bolshov,[32] D. Bortoletto,[47] J. Boudreau,[46] A. Boveia,[10] B. Brau,[10] A. Bridgeman,[24] L. Brigliadori,[5] C. Bromberg,[35] E. Brubaker,[13] J. Budagov,[15] H.S. Budd,[48] S. Budd,[24] K. Burkett,[17] G. Busetto,[42] P. Bussey,[21] A. Buzatu,[33] K. L. Byrum,[2] S. Cabrera[r],[16] M. Campanelli,[35] M. Campbell,[34] F. Canelli,[17] A. Canepa,[44] D. Carlsmith,[58] R. Carosi,[45] S. Carrillo[l],[18] S. Carron,[33] B. Casal,[11] M. Casarsa,[17] A. Castro,[5] P. Catastini,[45] D. Cauz,[53] M. Cavalli-Sforza,[3] A. Cerri,[28] L. Cerrito[p],[30] S.H. Chang,[27] Y.C. Chen,[1] M. Chertok,[7] G. Chiarelli,[45] G. Chlachidze,[17] F. Chlebana,[17] K. Cho,[27] D. Chokheli,[15] J.P. Chou,[22] G. Choudalakis,[32] S.H. Chuang,[51] K. Chung,[12] W.H. Chung,[58] Y.S. Chung,[48] C.I. Ciobanu,[24] M.A. Ciocci,[45] A. Clark,[20] D. Clark,[6] G. Compostella,[42] M.E. Convery,[17] J. Conway,[7] B. Cooper,[30] K. Copic,[34] M. Cordelli,[19] G. Cortiana,[42] F. Crescioli,[45] C. Cuenca Almenar[r],[7] J. Cuevas[o],[11] R. Culbertson,[17] J.C. Cully,[34] D. Dagenhart,[17] M. Datta,[17] T. Davies,[21] P. de Barbaro,[48] S. De Cecco,[50] A. Deisher,[28] G. De Lentdecker[d],[48] G. De Lorenzo,[3] M. Dell'Orso,[45] L. Demortier,[49] J. Deng,[16] M. Deninno,[5] D. De Pedis,[50] P.F. Derwent,[17] G.P. Di Giovanni,[43] C. Dionisi,[50] B. Di Ruzza,[53] J.R. Dittmann,[4] M. D'Onofrio,[3] S. Donati,[45] P. Dong,[8] J. Donini,[42] T. Dorigo,[42] S. Dube,[51] J. Efron,[38] R. Erbacher,[7] D. Errede,[24] S. Errede,[24] R. Eusebi,[17] H.C. Fang,[28] S. Farrington,[29] W.T. Fedorko,[13] R.G. Feild,[59] M. Feindt,[26] J.P. Fernandez,[31] C. Ferrazza,[45] R. Field,[18] G. Flanagan,[47] R. Forrest,[7] S. Forrester,[7] M. Franklin,[22] J.C. Freeman,[28] I. Furic,[18] M. Gallinaro,[49] J. Galyardt,[12] F. Garberson,[10] J.E. Garcia,[45] A.F. Garfinkel,[47] H. Gerberich,[24] D. Gerdes,[34] S. Giagu,[50] V. Giakoumopolou[a],[45] P. Giannetti,[45] K. Gibson,[46] J.L. Gimmell,[48] C.M. Ginsburg,[17] N. Giokaris[a],[15] M. Giordani,[53] P. Giromini,[19] M. Giunta,[45] V. Glagolev,[15] D. Glenzinski,[17] M. Gold,[36] N. Goldschmidt,[18] A. Golossanov,[17] G. Gomez,[11] G. Gomez-Ceballos,[32] M. Goncharov,[52] O. González,[31] I. Gorelov,[36] A.T. Goshaw,[16] K. Goulianos,[49] A. Gresele,[42] S. Grinstein,[22] C. Grosso-Pilcher,[13] R.C. Group,[17] U. Grundler,[24] J. Guimaraes da Costa,[22] Z. Gunay-Unalan,[35] C. Haber,[28] K. Hahn,[32] S.R. Hahn,[17] E. Halkiadakis,[51] A. Hamilton,[20] B.-Y. Han,[48] J.Y. Han,[48] R. Handler,[58] F. Happacher,[19] K. Hara,[54] D. Hare,[51] M. Hare,[55] S. Harper,[41] R.F. Harr,[57] R.M. Harris,[17] M. Hartz,[46] K. Hatakeyama,[49] J. Hauser,[8] C. Hays,[41] M. Heck,[26] A. Heijboer,[44] B. Heinemann,[28] J. Heinrich,[44] C. Henderson,[32] M. Herndon,[58] J. Heuser,[26] S. Hewamanage,[4] D. Hidas,[16] C.S. Hill[c],[10] D. Hirschbuehl,[26] A. Hocker,[17] S. Hou,[1] M. Houlden,[29] S.-C. Hsu,[9] B.T. Huffman,[41] R.E. Hughes,[38] U. Husemann,[59] J. Huston,[35] J. Incandela,[10] G. Introzzi,[45] M. Iori,[50] A. Ivanov,[7] B. Iyutin,[32] E. James,[17] B. Jayatilaka,[16] D. Jeans,[50] E.J. Jeon,[27] S. Jindariani,[18] W. Johnson,[7] M. Jones,[47] K.K. Joo,[27] S.Y. Jun,[12] J.E. Jung,[27] T.R. Junk,[24] T. Kamon,[52] D. Kar,[18] P.E. Karchin,[57] Y. Kato,[40] R. Kephart,[17] U. Kerzel,[26] V. Khotilovich,[52] B. Kilminster,[38] D.H. Kim,[27] H.S. Kim,[27] J.E. Kim,[27] M.J. Kim,[17] S.B. Kim,[27] S.H. Kim,[54] Y.K. Kim,[13] N. Kimura,[54] L. Kirsch,[6] S. Klimenko,[18] M. Klute,[32] B. Knuteson,[32] B.R. Ko,[16] S.A. Koay,[10] K. Kondo,[56] D.J. Kong,[27] J. Konigsberg,[18] A. Korytov,[18] A.V. Kotwal,[16] J. Kraus,[24] M. Kreps,[26] J. Kroll,[44] N. Krumnack,[4] M. Kruse,[16] V. Krutelyov,[10] T. Kubo,[54] S. E. Kuhlmann,[2] T. Kuhr,[26] N.P. Kulkarni,[57] Y. Kusakabe,[56] S. Kwang,[13] A.T. Laasanen,[47] S. Lai,[33] S. Lami,[45] S. Lammel,[17] M. Lancaster,[30] R.L. Lander,[7] K. Lannon,[38] A. Lath,[51] G. Latino,[45] I. Lazzizzera,[42] T. LeCompte,[2] J. Lee,[48] J. Lee,[27] Y.J. Lee,[27] S.W. Lee[q],[52] R. Lefèvre,[20] N. Leonardo,[32] S. Leone,[45] S. Levy,[13] J.D. Lewis,[17] C. Lin,[59] C.S. Lin,[28] J. Linacre,[41] M. Lindgren,[17] E. Lipeles,[9] A. Lister,[7] D.O. Litvintsev,[17] T. Liu,[17] N.S. Lockyer,[44] A. Loginov,[59] M. Loreti,[42] L. Lovas,[14] R.-S. Lu,[1] D. Lucchesi,[42] J. Lueck,[26] C. Luci,[50] P. Lujan,[28] P. Lukens,[17] G. Lungu,[18] L. Lyons,[41] J. Lys,[28] R. Lysak,[14] E. Lytken,[47] P. Mack,[26] D. MacQueen,[33] R. Madrak,[17] K. Maeshima,[17] K. Makhoul,[32] T. Maki,[23] P. Maksimovic,[25] S. Malde,[41] S. Malik,[30] G. Manca,[29] A. Manousakis[a],[15] F. Margaroli,[47] C. Marino,[26] C.P. Marino,[24] A. Martin,[59] M. Martin,[25] V. Martin[j],[21] M. Martínez,[3] R. Martínez-Ballarín,[31] T. Maruyama,[54] P. Mastrandrea,[50] T. Masubuchi,[54] M.E. Mattson,[57] P. Mazzanti,[5] K.S. McFarland,[48] P. McIntyre,[52] R. McNulty[i],[29] A. Mehta,[29] P. Mehtala,[23] S. Menzemer[k],[11] A. Menzione,[45] P. Merkel,[47] C. Mesropian,[49] A. Messina,[35] T. Miao,[17] N. Miladinovic,[6] J. Miles,[32] R. Miller,[35] C. Mills,[22] M. Milnik,[26] A. Mitra,[1] G. Mitselmakher,[18] H. Miyake,[54] S. Moed,[22] N. Moggi,[5] C.S. Moon,[27] R. Moore,[17] M. Morello,[45] P. Movilla Fernandez,[28] J. Mülmenstädt,[28]

A. Mukherjee,[17] Th. Muller,[26] R. Mumford,[25] P. Murat,[17] M. Mussini,[5] J. Nachtman,[17] Y. Nagai,[54] A. Nagano,[54] J. Naganoma,[56] K. Nakamura,[54] I. Nakano,[39] A. Napier,[55] V. Necula,[16] C. Neu,[44] M.S. Neubauer,[24] J. Nielsen[f],[28] L. Nodulman,[2] M. Norman,[9] O. Norniella,[24] E. Nurse,[30] S.H. Oh,[16] Y.D. Oh,[27] I. Oksuzian,[18] T. Okusawa,[40] R. Oldeman,[29] R. Orava,[23] K. Osterberg,[23] S. Pagan Griso,[42] C. Pagliarone,[45] E. Palencia,[17] V. Papadimitriou,[17] A. Papaikonomou,[26] A.A. Paramonov,[13] B. Parks,[38] S. Pashapour,[33] J. Patrick,[17] G. Pauletta,[53] M. Paulini,[12] C. Paus,[32] D.E. Pellett,[7] A. Penzo,[53] T.J. Phillips,[16] G. Piacentino,[45] J. Piedra,[43] L. Pinera,[18] K. Pitts,[24] C. Plager,[8] L. Pondrom,[58] X. Portell,[3] O. Poukhov,[15] N. Pounder,[41] F. Prakoshyn,[15] A. Pronko,[17] J. Proudfoot,[2] F. Ptohos[h],[17] G. Punzi,[45] J. Pursley,[58] J. Rademacker[c],[41] A. Rahaman,[46] V. Ramakrishnan,[58] N. Ranjan,[47] I. Redondo,[31] B. Reisert,[17] V. Rekovic,[36] P. Renton,[41] M. Rescigno,[50] S. Richter,[26] F. Rimondi,[5] L. Ristori,[45] A. Robson,[21] T. Rodrigo,[11] E. Rogers,[24] S. Rolli,[55] R. Roser,[17] M. Rossi,[53] R. Rossin,[10] P. Roy,[33] A. Ruiz,[11] J. Russ,[12] V. Rusu,[17] H. Saarikko,[23] A. Safonov,[52] W.K. Sakumoto,[48] G. Salamanna,[50] O. Saltó,[3] L. Santi,[53] S. Sarkar,[50] L. Sartori,[45] K. Sato,[17] A. Savoy-Navarro,[43] T. Scheidle,[26] P. Schlabach,[17] E.E. Schmidt,[17] M.A. Schmidt,[13] M.P. Schmidt,[59] M. Schmitt,[37] T. Schwarz,[7] L. Scodellaro,[11] A.L. Scott,[10] A. Scribano,[45] F. Scuri,[45] A. Sedov,[47] S. Seidel,[36] Y. Seiya,[40] A. Semenov,[15] L. Sexton-Kennedy,[17] A. Sfyria,[20] S.Z. Shalhout,[57] M.D. Shapiro,[28] T. Shears,[29] P.F. Shepard,[46] D. Sherman,[22] M. Shimojima[n],[54] M. Shochet,[13] Y. Shon,[58] I. Shreyber,[20] A. Sidoti,[45] P. Sinervo,[33] A. Sisakyan,[15] A.J. Slaughter,[17] J. Slaunwhite,[38] K. Sliwa,[55] J.R. Smith,[7] F.D. Snider,[17] R. Snihur,[33] M. Soderberg,[34] A. Soha,[7] S. Somalwar,[51] V. Sorin,[35] J. Spalding,[17] F. Spinella,[45] T. Spreitzer,[33] P. Squillacioti,[45] M. Stanitzki,[59] R. St. Denis,[21] B. Stelzer,[8] O. Stelzer-Chilton,[41] D. Stentz,[37] J. Strologas,[36] D. Stuart,[10] J.S. Suh,[27] A. Sukhanov,[18] H. Sun,[55] I. Suslov,[15] T. Suzuki,[54] A. Taffard[e],[24] R. Takashima,[39] Y. Takeuchi,[54] R. Tanaka,[39] M. Tecchio,[34] P.K. Teng,[1] K. Terashi,[49] J. Thom[g],[17] A.S. Thompson,[21] G.A. Thompson,[24] E. Thomson,[44] P. Tipton,[59] V. Tiwari,[12] S. Tkaczyk,[17] D. Toback,[52] S. Tokar,[14] K. Tollefson,[35] T. Tomura,[54] D. Tonelli,[17] S. Torre,[19] D. Torretta,[17] S. Tourneur,[43] W. Trischuk,[33] Y. Tu,[44] N. Turini,[45] F. Ukegawa,[54] S. Uozumi,[54] S. Vallecorsa,[20] N. van Remortel,[23] A. Varganov,[34] E. Vataga,[36] F. Vázquez[l],[18] G. Velev,[17] C. Vellidis[a],[45] V. Veszpremi,[47] M. Vidal,[31] R. Vidal,[17] I. Vila,[11] R. Vilar,[11] T. Vine,[30] M. Vogel,[36] I. Volobouev[q],[28] G. Volpi,[45] F. Würthwein,[9] P. Wagner,[44] R.G. Wagner,[2] R.L. Wagner,[17] J. Wagner-Kuhr,[26] W. Wagner,[26] T. Wakisaka,[40] R. Wallny,[8] S.M. Wang,[1] A. Warburton,[33] D. Waters,[30] M. Weinberger,[52] W.C. Wester III,[17] B. Whitehouse,[55] D. Whiteson[e],[44] A.B. Wicklund,[2] E. Wicklund,[17] G. Williams,[33] H.H. Williams,[44] P. Wilson,[17] B.L. Winer,[38] P. Wittich[g],[17] S. Wolbers,[17] C. Wolfe,[13] T. Wright,[34] X. Wu,[20] S.M. Wynne,[29] A. Yagil,[9] K. Yamamoto,[40] J. Yamaoka,[51] T. Yamashita,[39] C. Yang,[59] U.K. Yang[m],[13] Y.C. Yang,[27] W.M. Yao,[28] G.P. Yeh,[17] J. Yoh,[17] K. Yorita,[13] T. Yoshida,[40] G.B. Yu,[48] I. Yu,[27] S.S. Yu,[17] J.C. Yun,[17] L. Zanello,[50] A. Zanetti,[53] I. Zaw,[22] X. Zhang,[24] Y. Zheng[b],[8] and S. Zucchelli[5]

(CDF Collaboration*)

[1]*Institute of Physics, Academia Sinica, Taipei, Taiwan 11529, Republic of China*
[2]*Argonne National Laboratory, Argonne, Illinois 60439*
[3]*Institut de Fisica d'Altes Energies, Universitat Autonoma de Barcelona, E-08193, Bellaterra (Barcelona), Spain*
[4]*Baylor University, Waco, Texas 76798*
[5]*Istituto Nazionale di Fisica Nucleare, University of Bologna, I-40127 Bologna, Italy*
[6]*Brandeis University, Waltham, Massachusetts 02254*
[7]*University of California, Davis, Davis, California 95616*
[8]*University of California, Los Angeles, Los Angeles, California 90024*
[9]*University of California, San Diego, La Jolla, California 92093*
[10]*University of California, Santa Barbara, Santa Barbara, California 93106*
[11]*Instituto de Fisica de Cantabria, CSIC-University of Cantabria, 39005 Santander, Spain*
[12]*Carnegie Mellon University, Pittsburgh, PA 15213*
[13]*Enrico Fermi Institute, University of Chicago, Chicago, Illinois 60637*
[14]*Comenius University, 842 48 Bratislava, Slovakia; Institute of Experimental Physics, 040 01 Kosice, Slovakia*
[15]*Joint Institute for Nuclear Research, RU-141980 Dubna, Russia*
[16]*Duke University, Durham, North Carolina 27708*
[17]*Fermi National Accelerator Laboratory, Batavia, Illinois 60510*
[18]*University of Florida, Gainesville, Florida 32611*
[19]*Laboratori Nazionali di Frascati, Istituto Nazionale di Fisica Nucleare, I-00044 Frascati, Italy*
[20]*University of Geneva, CH-1211 Geneva 4, Switzerland*
[21]*Glasgow University, Glasgow G12 8QQ, United Kingdom*
[22]*Harvard University, Cambridge, Massachusetts 02138*
[23]*Division of High Energy Physics, Department of Physics,*
University of Helsinki and Helsinki Institute of Physics, FIN-00014, Helsinki, Finland

[24]University of Illinois, Urbana, Illinois 61801
[25]The Johns Hopkins University, Baltimore, Maryland 21218
[26]Institut für Experimentelle Kernphysik, Universität Karlsruhe, 76128 Karlsruhe, Germany
[27]Center for High Energy Physics: Kyungpook National University, Daegu 702-701, Korea; Seoul National University, Seoul 151-742, Korea; Sungkyunkwan University, Suwon 440-746, Korea; Korea Institute of Science and Technology Information, Daejeon, 305-806, Korea; Chonnam National University, Gwangju, 500-757, Korea
[28]Ernest Orlando Lawrence Berkeley National Laboratory, Berkeley, California 94720
[29]University of Liverpool, Liverpool L69 7ZE, United Kingdom
[30]University College London, London WC1E 6BT, United Kingdom
[31]Centro de Investigaciones Energeticas Medioambientales y Tecnologicas, E-28040 Madrid, Spain
[32]Massachusetts Institute of Technology, Cambridge, Massachusetts 02139
[33]Institute of Particle Physics: McGill University, Montréal, Canada H3A 2T8; and University of Toronto, Toronto, Canada M5S 1A7
[34]University of Michigan, Ann Arbor, Michigan 48109
[35]Michigan State University, East Lansing, Michigan 48824
[36]University of New Mexico, Albuquerque, New Mexico 87131
[37]Northwestern University, Evanston, Illinois 60208
[38]The Ohio State University, Columbus, Ohio 43210
[39]Okayama University, Okayama 700-8530, Japan
[40]Osaka City University, Osaka 588, Japan
[41]University of Oxford, Oxford OX1 3RH, United Kingdom
[42]University of Padova, Istituto Nazionale di Fisica Nucleare, Sezione di Padova-Trento, I-35131 Padova, Italy
[43]LPNHE, Universite Pierre et Marie Curie/IN2P3-CNRS, UMR7585, Paris, F-75252 France
[44]University of Pennsylvania, Philadelphia, Pennsylvania 19104
[45]Istituto Nazionale di Fisica Nucleare Pisa, Universities of Pisa, Siena and Scuola Normale Superiore, I-56127 Pisa, Italy
[46]University of Pittsburgh, Pittsburgh, Pennsylvania 15260
[47]Purdue University, West Lafayette, Indiana 47907
[48]University of Rochester, Rochester, New York 14627
[49]The Rockefeller University, New York, New York 10021
[50]Istituto Nazionale di Fisica Nucleare, Sezione di Roma 1, University of Rome "La Sapienza," I-00185 Roma, Italy
[51]Rutgers University, Piscataway, New Jersey 08855
[52]Texas A&M University, College Station, Texas 77843
[53]Istituto Nazionale di Fisica Nucleare, University of Trieste/ Udine, Italy
[54]University of Tsukuba, Tsukuba, Ibaraki 305, Japan
[55]Tufts University, Medford, Massachusetts 02155
[56]Waseda University, Tokyo 169, Japan
[57]Wayne State University, Detroit, Michigan 48201
[58]University of Wisconsin, Madison, Wisconsin 53706
[59]Yale University, New Haven, Connecticut 06520

(Dated: October 22, 2007)

A direct measurement of the total decay width of the W boson Γ_W is presented using 350 pb^{-1} of data from $p\overline{p}$ collisions at $\sqrt{s} = 1.96$ TeV collected with the CDF II detector at the Fermilab Tevatron. The width is determined by normalizing predicted signal and background distributions to 230185 W candidates decaying to $e\nu$ and $\mu\nu$ in the transverse-mass region $50 < M_T < 90$ GeV and then fitting the predicted shape to 6055 events in the high-M_T region, $90 < M_T < 200$ GeV. The result is $\Gamma_W = 2032 \pm 45$ (stat.) ± 57 (syst.) MeV, consistent with the standard model expectation.

PACS numbers: 13.38.Be, 14.70.Fm

*With visitors from [a]University of Athens, 15784 Athens, Greece, [b]Chinese Academy of Sciences, Beijing 100864, China, [c]University of Bristol, Bristol BS8 1TL, UK, [d]University Libre de Bruxelles, B-1050 Brussels, Belgium, [e]University of California Irvine, Irvine, CA 92697, [f]University of California Santa Cruz, Santa Cruz, CA 95064, [g]Cornell University, Ithaca, NY 14853, [h]University of Cyprus, Nicosia CY-1678, Cyprus, [i]University College Dublin, Dublin 4, Ireland, [j]University of Edinburgh, Edinburgh EH9 3JZ,

The decay widths of the W and Z bosons that mediate the weak interaction are precisely predicted within the standard model (SM). At Born level the W width Γ_W and mass M_W are related through the precisely determined Fermi coupling constant, G_F. Beyond leading order, higher-order electroweak (EW) and quantum-chromodynamic (QCD) corrections, $\delta_{EW} \approx -0.4\%$ and $\delta_{QCD} \approx 2.5\%$ respectively, modify the relation such that $\Gamma_W = \frac{3G_F M_W^3}{\sqrt{8}\pi}(1 + \delta_{EW} + \delta_{QCD})$ [1]. The uncertainty on the SM prediction $\Gamma_W = 2091 \pm 2$ MeV is dominated by the uncertainty on M_W with smaller contributions from the uncertainties on the higher order corrections [2]. Uncertainties on SM parameters, such as the Higgs boson mass, affect this prediction very weakly, and so a measurement allows an unambiguous test of the SM that can also be used to constrain other SM parameters such as the V_{cs} CKM matrix element [3]. The average of previously published direct measurements of Γ_W from $p\overline{p}$ collisions at the Tevatron [4] and e^+e^- collisions at LEP-II [5] has a combined uncertainty of 2.7% with the most precise determination from a single experiment (ALEPH) having an uncertainty of 5.1%. The most precise indirect determination [6] of Γ_W from a measurement of the ratio $R = \frac{\sigma(p\overline{p}\to W\to \ell\nu)}{\sigma(p\overline{p}\to Z\to \ell^+\ell^-)}$ has an uncertainty of 2%.

This Letter presents the world's most precise direct determination of Γ_W from a single experiment. The analysis uses $W \to e\nu$ and $W \to \mu\nu$ data with respective integrated luminosities of 370 pb^{-1} and 330 pb^{-1} collected by the CDF II detector at the Fermilab Tevatron.

Neutrinos are undetectable by the CDF II detector and hence the invariant mass of the W boson cannot be reconstructed. Γ_W is therefore determined from a fit to the distribution of the W transverse mass $M_T = \sqrt{2\left(p_T^\ell p_T^\nu - \vec{p}_T^{\,\ell} \cdot \vec{p}_T^{\,\nu}\right)}$, where $\vec{p}_T^{\,\ell}$ and $\vec{p}_T^{\,\nu}$ are the measured transverse momentum of the charged lepton and the transverse momentum of the neutrino as inferred from the observed missing transverse energy, respectively. Events with $M_T > M_W$ arise predominantly from a combination of non-zero W width and finite detector resolution. A precise Γ_W measurement from the $M_T > M_W$ events is possible because the width component of the high-M_T line-shape falls off more slowly than the resolution component.

The components of the CDF II detector relevant to this analysis are described briefly here; a more complete description can be found elsewhere [7]. A silicon microstrip detector [8] is used to measure the distance of closest approach in the transverse plane, d_0, of charged particles to the beamline. The momenta of charged particles are measured using a 96-layer open-cell drift chamber (COT) [9] inside a 1.4 T solenoid. Optimal p_T resolution is obtained by constraining trajectories to originate from the beamline. Electromagnetic and hadronic calorimeters, arranged in a projective tower geometry, cover the pseudorapidity range $|\eta| < 3.64$ [10]. In the region $|\eta| < 1.0$, a lead/scintillator electromagnetic calorimeter (CEM) [11] measures electron energies and proportional chambers embedded at the shower maximum provide further information on shower shapes and positions. A system of drift chambers, scintillators, and steel absorbers outside the calorimeters is used to identify muons in the region $|\eta| < 1.0$ [12].

$W \to e\nu$ candidate events are selected by a large transverse energy electron trigger, and the electron shower is required to have transverse energy $E_T^e > 25$ GeV [10] in the CEM. The ratio of the energy measured in the CEM and the charged-track momentum measured in the COT, E/p, must satisfy $0.8 < E/p < 1.3$. The ratio of energy deposited in the hadronic (HAD) and CEM calorimeter towers is required to satisfy $E_{\mathrm{HAD}}/E_{\mathrm{CEM}} < 0.07$. The electron shower must be contained within a fiducial region of the CEM, away from calorimeter cell boundaries, and must have a typical electron lateral shower profile on the projection of the COT track in the CEM. Contamination by $Z \to e^+e^-$ events is reduced by rejecting events with an additional high p_T track of opposite sign charge pointing to an un-instrumented region of the calorimeter.

$W \to \mu\nu$ candidate events are selected by a large p_T muon trigger and are required to contain a COT track, well matched to a track segment in the muon chambers, with transverse momentum $p_T^\mu > 25$ GeV. The energy deposited in the electromagnetic and hadronic calorimeters must be consistent with the passage of a minimum-ionizing particle. Requirements on the track d_0 and χ^2 are imposed to reject background. Events consistent with cosmic rays or those with an additional high-p_T track consistent with $Z \to \mu^+\mu^-$ decays are removed.

The existence of a neutrino is inferred from a transverse momentum imbalance. The missing transverse momentum, $\vec{p}_T^{\,\nu} \equiv -\left(\vec{p}_T^{\,\ell} + \vec{u}\right)$, must satisfy $p_T^\nu > 25$ GeV. The components of the recoil transverse energy vector $\vec{u}$ are defined as $\sum_i E_i \sin\theta_i(\cos\phi_i, \sin\phi_i)$, for calorimeter towers i with $|\eta| < 3.64$, excluding those traversed by and surrounding the charged lepton. $\vec{u}$ receives contributions from initial-state QCD radiation, underlying-event energy, final-state photon radiation, and overlapping $p\overline{p}$ interactions. To reduce backgrounds and improve transverse mass resolution, the recoil energy must satisfy $u < 20$ GeV. The $W \to e\nu$ ($W \to \mu\nu$) sample consists of 127432 (108808) candidate events in the range $50 < M_T < 200$ GeV and 3436 (2619) in the high M_T range of $90 < M_T < 200$ GeV.

UK, [k]University of Heidelberg, D-69120 Heidelberg, Germany, [l]Universidad Iberoamericana, Mexico D.F., Mexico, [m]University of Manchester, Manchester M13 9PL, UK, [n]Nagasaki Institute of Applied Science, Nagasaki, Japan, [o]University de Oviedo, E-33007 Oviedo, Spain, [p]Queen Mary, University of London, London E1 4NS, UK, [q]Texas Tech University, Lubbock, TX 79409, [r]IFIC(CSIC-Universitat de Valencia), 46071 Valencia, Spain,

Since the W and Z bosons share a common production mechanism and the momenta of Z bosons can be directly reconstructed from their decay products, $Z \to \ell^+\ell^-$ decays are used to model the detector's response to $W \to \ell\nu$ events. Samples of $Z \to e^+e^-$ and $Z \to \mu^+\mu^-$ candidates are selected by requiring two charged leptons, with the same requirements as the $W \to \ell\nu$ candidates, with the exception that the muon chamber track match requirement is removed for one of the muons in the $Z \to \mu^+\mu^-$ pair. The di-lepton invariant mass is required to satisfy $80 < M^{\ell\ell} < 100$ GeV. Samples of 2909 $Z \to e^+e^-$ and 6271 $Z \to \mu^+\mu^-$ events with recoil energy $u < 20$ GeV are used to determine the scale and resolution of the lepton energy and momentum measurements. A second set of $Z \to e^+e^-$ and $Z \to \mu^+\mu^-$ control samples is defined with the u cut replaced by a di-lepton transverse momentum cut, $p_T^{\ell\ell} < 50$ GeV, in order to constrain the W boson's transverse momentum spectrum and to provide an empirical model of the recoil.

The W boson M_T spectrum is modeled using a Monte-Carlo simulation. The CTEQ6M [13] parton distribution functions (PDFs) are used, and W boson invariant masses $\sqrt{\hat{s}}$ are generated according to an energy-dependent Breit-Wigner distribution: $\sigma(\hat{s}) \sim \left[\hat{s}\left(1 - M_W^2/\hat{s}\right)^2 + \hat{s}\Gamma_W^2/M_W^2\right]^{-1}$. Higher order QCD effects are included by generating the W bosons with a p_T distribution from a NLO combined with resummation QCD calculation [14] with the non-perturbative prescription of [15]. Photon radiation from the charged lepton is simulated using a $\mathcal{O}(\alpha)$ matrix-element calculation [16]. Corrections for EW box diagrams are applied from the calculation of [17].

The charged leptons and radiated photons are passed through a detailed detector simulation that models the energy loss due to ionization and bremsstrahlung. The simulation also includes a parametric model of the $\vec{u}$ measurement as a function of the boson p_T. The same kinematic and geometric cuts used to select candidate events in the data are applied to the simulation. The simulation produces M_T spectra for Γ_W values ranging from 1.0 to 3.0 GeV with M_W fixed at 80.403 GeV.

This measurement relies on the accurate modeling of the M_T distribution over a wide range. The most important sources of systematic uncertainty affecting the M_T shape arise from the charged-lepton energy and momentum scales and resolutions, the recoil modeling, and the presence of backgrounds. All systematic uncertainties are evaluated by varying parameters in the simulation and then fitting the resulting M_T spectra with the nominal spectra. Uncertainties have been calculated separately for the fit region $M_T^{\mathrm{cut}} < M_T < 200$ GeV for M_T^{cut} values ranging from 80 to 110 GeV. While the statistical uncertainty decreases as M_T^{cut} is lowered, the systematic uncertainty increases. A value of $M_T^{\mathrm{cut}} = 90$ GeV gives the smallest total uncertainty. Backgrounds are added to the simulation M_T spectra which are then normalized to the number of data events in the region $50 < M_T < 90$ GeV.

The COT momentum scale is determined from a fit to the $Z \to \mu^+\mu^-$ invariant mass distribution with the Z mass constrained to the world average value [2]. A consistent COT momentum scale is obtained from fits to the invariant mass distributions of $J/\psi \to \mu^+\mu^-$ and $\Upsilon \to \mu^+\mu^-$ events [7]. The difference between the three determinations has a negligible effect on this analysis. The contribution to the uncertainty on Γ_W in the $W \to \mu\nu$ channel $\Delta\Gamma_W^{\mu\nu}$ arising from the 0.04% uncertainty in the COT momentum scale, due to the $Z \to \mu^+\mu^-$ statistics, is $\Delta\Gamma_W^{\mu\nu} = 17$ MeV.

By scaling the resolutions predicted by a GEANT [18] simulation of the COT to match the observed di-muon invariant mass in $Z \to \mu^+\mu^-$ decays, we obtain a momentum resolution of $\sigma(1/p_T) = (5.4 \pm 0.2) \times 10^{-4}$ GeV^{-1}. A consistent $\sigma(1/p_T)$ is also determined using the E/p distribution of the $W \to e\nu$ data. The combined uncertainties from the $Z \to \mu^+\mu^-$ and E/p fits for the COT resolution give $\Delta\Gamma_W^{\mu\nu} = 26$ MeV.

The CEM energy scale and resolution are determined from fits to the $Z \to e^+e^-$ invariant-mass distribution with the Z mass constrained to the world average value [2] and to the E/p distribution of electrons in $W \to e\nu$ events, using the calibration of p described above. The scales determined from the two methods are consistent and are combined to form a weighted average with an uncertainty of 0.04%. The contribution to the uncertainty on Γ_W in the $W \to e\nu$ channel $\Delta\Gamma_W^{e\nu}$ arising from this uncertainty is $\Delta\Gamma_W^{e\nu} = 17$ MeV.

The CEM resolution fits constrain the constant term κ in the CEM resolution function $\sigma(E)/E = 13.5\%/\sqrt{E_T(\mathrm{GeV})} \oplus \kappa$ [11]. The E/p and $Z \to e^+e^-$ fit results differ by 1.6 standard deviations. They are combined and an uncertainty is assigned that spans both values, as well as the values obtained when the E/p fit region is varied, to give $\kappa = 1.1 \pm 0.4\%$. This uncertainty on the CEM resolution gives $\Delta\Gamma_W^{e\nu} = 31$ MeV.

Energy loss by electrons and photons in the solenoid coil and associated material prior to the CEM, as well as energy leakage into the hadronic calorimeter, are parameterized based on the results of a GEANT simulation, and input into our simulation. In addition to these simulated sources of CEM non-linearity, an additional per-particle intrinsic non-linearity is determined from the $W \to e\nu$ and $Z \to e^+e^-$ data by fitting the E/p distribution in bins of E_T. Its uncertainty gives $\Delta\Gamma_W^{e\nu} = 12$ MeV, resulting in a total uncertainty of 21 MeV on $\Gamma_W^{e\nu}$ from the uncertainties on the electron energy scale determination. Finally, uncertainties in the modeling of very low-energy photons and the amount of passive material prior to the COT give $\Delta\Gamma_W^{e\nu} = 13$ MeV.

The recoil transverse energy vector $\vec{u}$ is used to determine $\vec{p}_T^{\,\nu}$ and hence M_T. Since $\vec{u}$ comes predominantly from initial-state QCD radiation, which is balanced by the W or Z boson p_T, we form an empirical model by parameterizing its response and resolution as a function of $p_T^{\ell\ell}$. The parameters of the model are varied according to the covariance matrices obtained in the fits to Z data. The resulting uncertainties on $\vec{u}$ from the recoil model give $\Delta\Gamma_W^{e\nu}$ ($\Delta\Gamma_W^{\mu\nu}$) = 54 (49) MeV. The uncertainty in the modeling of the p_T^W distribution is determined by fitting the $p_T^{\ell\ell}$ distribution in $Z \to \ell^+\ell^-$ decays and results in a 7 MeV common uncertainty on Γ_W.

Several background processes can mimic the W signal. The process $W \to \tau\nu \to \ell\nu\nu\nu$ has a signature similar to $W \to \ell\nu$ decays, but with lower M_T. $Z \to \ell^+\ell^-$ events, where only one lepton is identified, can be reconstructed as W candidates. These two backgrounds can be accurately simulated and their contribution to the W signal is determined from Monte-Carlo simulation. QCD multi-jet backgrounds arise when one jet mimics a charged lepton and another is mismeasured to produce an energy imbalance. Since the region with apparently low p_T^ν is enriched in QCD background, the background normalization is estimated from a fit to the p_T^ν distribution in events where the p_T^ν and low M_T cut are not applied. The background p_T^ν spectrum is taken from data events in which some of the charged-lepton identification cuts have been reversed, and the signal spectrum is taken from the simulation. A decay-in-flight (DIF) background to the $W \to \mu\nu$ signal arises when kaons or pions decay to $\mu\nu$ inside the COT. The resulting kink in the track curvature may cause an overestimate of muon momentum, a transverse momentum imbalance, and a large χ^2 value between the COT hits assigned to the track and the fitted track trajectory. This background is estimated from a fit to the χ^2 distribution. The background spectrum is taken from events with a large d_0 and the signal from $Z \to \mu^+\mu^-$ events, which have negligible background. The total background fraction in the $90 < M_T < 200$ GeV fit region is 4.0±0.2% (10.8±0.3%) in the electron (muon) channel. Varying the background predictions within their normalization uncertainties, as well as varying their M_T shapes, causes variations in the electron (muon) Γ_W of 32 (33) MeV. The backgrounds that contribute the most to the width uncertainty are the QCD multijet background in the electron channel and the DIF background in the muon channel.

We also investigate small systematic uncertainties due to PDFs, M_W, EW corrections, lepton identification, and acceptance. The uncertainty on Γ_W arising from PDFs is determined using the variations defined by the CTEQ6M PDF eigenvector basis [13]. The PDF error sets span a 90% confidence interval so the resulting Γ_W shifts are divided by 1.6 to obtain 1σ uncertainties [19], giving an uncertainty of 16 MeV in both channels. A systematic uncertainty of 12 MeV is added in quadrature to this to account for the effect of higher order QCD effects not implemented in the Monte-Carlo simulation which was estimated from a comparison of the width obtained using NLO and NNLO PDFs [20]. Varying M_W by the uncertainty of ±29 MeV [2] from the central value of 80.403 GeV changes Γ_W by ∓9 MeV in each channel.

The impact of higher-order EW corrections is determined by comparing the $W \to \ell\nu\gamma$ and $W \to \ell\nu\gamma\gamma$ processes with the PHOTOS [21] simulation. Uncertainties on $\Gamma_W^{e\nu}$ ($\Gamma_W^{\mu\nu}$) of 8 (1) MeV were obtained. The impact of EW box diagrams was determined to be 12 MeV in both channels. A systematic uncertainty of 6 MeV in the box diagram correction was assigned from the dependence of the correction on the recoil resolution. The uncertainty in simulating lepton identification variables was constrained from $Z \to \ell^+\ell^-$ decays and results in a Γ_W uncertainty of 10 (6) MeV in the electron (muon) channel. Variations in the simulation of the detector acceptance results in an additional small uncertainty of 3 (4) MeV in the electron (muon) channel. Table I summarizes the sources of uncertainty described above.

A binned likelihood fit to simulated M_T spectra with Γ_W as a free parameter over the region $90 < M_T < 200$ GeV gives $\Gamma_W = 2118 \pm 60$ (stat.) MeV for the electron channel and $\Gamma_W = 1948 \pm 67$ (stat.) MeV for the muon channel. Figure 1 shows the M_T distributions of the data with the best fits. The electron and muon results have a common uncertainty of 27 MeV and are combined using the BLUE method [22] to give $\Gamma_W = 2032 \pm 45$ (stat.) ± 57 (syst.) MeV. The combination has a χ^2 of 1.6 and a total uncertainty of 73 MeV. No statistically significant difference is found between fits using only positively and only negatively charged leptons. As a cross-check, the W width was also determined from a fit to the charged-lepton transverse momentum, which has a different sensitivity to many of the systematics, and a value of Γ_W consistent with the M_T fit was obtained.

The result presented in this Letter is the most precise direct measurement of the W width. It can be combined with published Tevatron direct width measurements [4] to give a hadron collider average of $\Gamma_W = 2057 \pm 62$ MeV. A further combination with the preliminary value obtained from e^+e^- collisions, $\Gamma_W = 2196 \pm 84$ MeV [23], gives a new world average value of $\Gamma_W = 2106 \pm 50$ MeV, in good agreement with the SM prediction.

We thank the Fermilab staff and the technical staffs of the participating institutions for their vital contributions. This work was supported by the U.S. Department of Energy and National Science Foundation; the Italian Istituto Nazionale di Fisica Nucleare; the Ministry of Education, Culture, Sports, Science and Technology of Japan; the Natural Sciences and Engineering Research Council of Canada; the National Science Council of the Republic of China; the Swiss National Science Foundation; the A.P. Sloan Foundation; the Bundesministerium für Bildung und Forschung, Germany; the Korean Science and Engineering Foundation and the Korean Research Foundation; the Science and Technology Facilities Council and the Royal Society, UK; the Institut National de Physique Nucleaire et Physique des Particules/CNRS;

TABLE I: The sources of uncertainty (in MeV) on Γ_W for the $W \to e\nu$ and $W \to \mu\nu$ measurements. If there is a correlated source of error between the two measurements its contribution to each measurement is listed in the third column, labeled C.

Source	$\Delta\Gamma_W^{e\nu}$	$\Delta\Gamma_W^{\mu\nu}$	C
Statistics	60	67	
Lepton E or p scale	21	17	12
Lepton E or p resolution	31	26	
Electron energy loss simulation	13		
Recoil model	54	49	
p_T^W	7	7	7
Backgrounds	32	33	
PDFs	20	20	20
M_W	9	9	9
EW radiative corrections	10	6	6
Lepton ID/acceptance	10	7	
Total Syst.	79	71	27
Total (Stat. + Syst.)	99	98	27

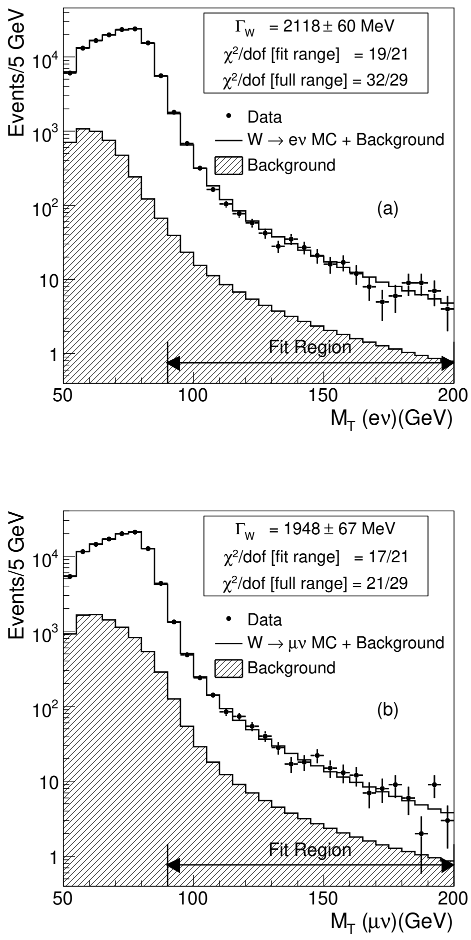

FIG. 1: The transverse mass distributions of the $W \to e\nu$ data (a) and $W \to \mu\nu$ data (b) compared to the best fit.

the Russian Foundation for Basic Research; the Comisión Interministerial de Ciencia y Tecnología, Spain; the European Community's Human Potential Programme; the Slovak R&D Agency; and the Academy of Finland.

[1] J. L. Rosner, M. P. Worah, and T. Takeuchi, Phys. Rev. D **49**, 1363 (1994).
[2] W.-M. Yao *et al.*, J. Phys. G **33**, 1 (2006).
[3] P. B. Renton, Rept. Prog. Phys. **65**, 1271 (2002).
[4] V. Abazov *et al.*, (CDF Collaboration, D0 Collaboration, Tevatron EW Working Group), Phys. Rev. D **70**, 092008 (2004).
[5] S. Schael *et al.* (ALEPH Collaboration), Eur. Phys. J. C **47**, 309 (2006); G. Abbiendi *et al.* (OPAL Collaboration), *ibid.* **45**, 307 (2006); P. Achard *et al.* (L3 Collaboration), *ibid.* **45**, 569 (2006); P.Abreu *et al.* (DELPHI Collaboration), Phys. Lett. B **511**, 159 (2001).
[6] D. Acosta *et al.* (CDF Collaboration), Phys. Rev. Lett. **94**, 091803 (2005).
[7] T. Aaltonen *et al.* (CDF Collaboration), arXiv:0708.3642 [hep-ex].
[8] A. Sill *et al.*, Nucl. Instrum. Methods A **447**, 1 (2000); A. Affolder *et al.*, *ibid.* **453**, 84 (2000).
[9] A. Affolder *et al.*, Nucl. Instrum. Methods A **526**, 249 (2004).
[10] Throughout this Letter units of $\hbar = c = 1$ are used such that momenta and masses are in units of MeV or GeV. CDF uses a cylindrical coordinate system in which ϕ is the azimuthal angle, θ is the polar angle, and z points in the proton beam direction. The pseudorapidity, η, is defined as $\eta \equiv -\ln\tan(\theta/2)$. The transverse plane is the plane perpendicular to the z axis. The transverse energy is defined to be $E_T = E\sin\theta$.
[11] L. Balka *et al.*, Nucl. Instrum. Methods A **267**, 272 (1988).
[12] G. Ascoli *et al.*, Nucl. Instrum. Methods A **268**, 33 (1998).
[13] J. Pumplin *et al.*, J. High Energy Phys. **0207**, 012 (2002).
[14] P. B. Arnold and R. P. Kaufman, Nucl. Phys. **B349**, 381 (1991); P. B. Arnold and M. H. Reno, *ibid.* **319**, 37 (1989); P. B. Arnold, R. K. Ellis, and M. H. Reno, Phys. Rev. D **40**, 912 (1989).
[15] F. Landry *et al.*, Phys. Rev. D **67**, 073016 (2003).
[16] F. A. Berends *et al.*, Z. Phys. C **27**, 155 (1985); F. A. Berends and R. Kleiss, *ibid.* **27**, 365 (1985).
[17] U. Baur and D. Wackeroth, Phys. Rev. D **70**, 073015 (2004).
[18] R. Brun and F. Carminati, CERN Program Library Long Writeup, W5013, 1993 (unpublished), version 3.15.
[19] J. M. Campbell, J. W. Huston, and W. J. Stirling, Rep. Prog. Phys. **70**, 89 (2007).
[20] A.D. Martin, R.G. Roberts, W.J. Stirling, and R.S. Thorne, Phys. Lett. B **604**, 61 (2004).
[21] E. Barberio and Z. Was, Comput. Phys. Commun. **79**, 291 (1994); E. Barberio, B. van Eijk, and Z. Was, *ibid.* **66**, 115 (1991).
[22] L. Lyons, D. Gibaut, and P. Clifford, Nucl. Instrum. Methods A **270**, 110 (1988).
[23] J. Alcaraz *et al.* (LEP Electroweak Working Group), arXiv:hep-ex/0612034.